and so the error on the stream velocity caused by the estimation of reference temperature is small. For instance, the stream velocity at the center of the arc is given as 124 m/sec when the arithmetic mean temperature 9000°K is used for a reference temperature, and the variation of this value is less than 10% when any temperature in the range from 4500° to 16,000°K is used for the reference temperature.

In the high temperature gas, the mean free path is long because of the low number density and small collision cross section. The mean free path of atmospheric argon defined by $(n_a\lambda_a + n_i\lambda_i)/(n_a + n_i)$ is 4.52×10^{-4} cm at 9000°K (reference temperature used at the center of the arc), and the corresponding Knudsen number, related to the length of side of the drag plate, is 2.83×10^{-3}. From this, it is assumed that no correction for slip flow is needed.

In the arc, besides the general plasma stream that is considered in this report, there exist the movements of electrons and ions as current carriers. It is assumed that their drag on the drag plate is negligible.

This method of stream velocity measurement is applicable only where the stream is parallel to the arc axis, because C_d shown in Fig. 8 is the value in the case where the flow is perpendicular to the drag plate. It is assumed that the stream in the arc column is nearly parallel to the arc axis, except in the neighborhood of electrodes, a result shown in Ref. 1.

In the evaluation of stream velocity by Eq. (4), the error in the density of the plasma is less than 10%, and the error in drag is less than 5%, and so the error in the stream velocity from these causes is less than 7.5%. Considering that the error in stream velocity caused by the estimation of the reference temperature will be less than 10%, the combined error in stream velocity is less than 17.5%. Not included is the error due to some change of the arc discharge caused by inserting the drag measuring plate. It is difficult to assess this error, however, and considering the motion picture record (Fig. 6), it is assumed not serious.

References

[1] Wienecke, R., "Über das geschwindigkeitsfeld der hochstromkohlebogensäule," Z. Physik **143**, 128–140 (1955).

[2] Reed, T. B., "Determination of streaming velocity and the flow of heat and mass in high-current arcs," J. Appl. Phys. **31**, 2048–2052 (1960).

[3] Larentz, W., "Über ein verfahren zur messung sehr hoher temperaturen in nahezu durchlässigen bogensäulen," Z. Physik **129**, 327–342 (1951).

[4] Olsen, H. N., "Thermal and electrical properties of an argon plasma," Phys. Fluids **2**, 614–623 (1959).

[5] Nestor, O. H. and Olsen, H. N., "Numerical methods for reducing line and surface probe data," Soc. Ind. Appl. Math. Rev. **2**, 200 (1960).

[6] McAdams, W. H., *Heat Transmission* (McGraw-Hill Book Co. Inc., New York, 1954), pp. 265–266.

[7] Olsen, H. N., "Measurement of argon transition probabilities using the thermal arc plasma as a radiation source," Quant. Spectroscopy Radiative Transfer (to be published).

[8] Chapman, S. and Cowling, T. G., *The Mathematical Theory of Non-uniform Gases* (Cambridge University Press, Cambridge, 1952), pp. 151–198.

[9] Jeans, J., *An Introduction to the Kinetic Theory of Gases* (Cambridge University Press, Cambridge, 1952), pp. 181–183.

FEBRUARY 1963 AIAA JOURNAL VOL. 1, NO. 2

Electrical Propulsion Capabilities for Lunar Exploration

Harold Brown* and Harry E. Nicoll Jr.†
General Electric Company, Evendale, Ohio

The logical result of a successful Apollo program can be expected to be a large scale operation involving manned lunar exploration and colonization. This paper will examine the potential role of electrical propulsion in such an operation. Primary emphasis is placed on the identification of mission capabilities for providing logistic support. Electrical engine and nuclear-mechanical power conversion system experience is projected to the 1 to 10 Mw range and used to identify expected system characteristics. Both thermal arc and ion engines are considered. A basic mission profile is defined, and typical trajectory characteristics are discussed. The low thrust characteristic velocity requirement for the basic mission is identified and used to generate parametric mission performance characteristics for one-way, round-trip, and multitrip missions. These data indicate the interrelationships between gross weight, power rating, specific impulse, and total propulsion time and their effect on payload capabilities. The resulting data then are compared with the capabilities of comparable chemical and nuclear rocket-propelled vehicles.

Nomenclature

a_3 = semimajor axis of initial lunar orbit, miles
e_1 = eccentricity of earth transfer orbit
E = eccentric anomaly of earth transfer orbit, rad
f = universal gravitational constant, $9.404(10)^{-14}$ miles³/lb-hr²
F = engine thrust, lb
g_0 = sea level gravitational constant, 79,019 miles/hr²
I_{sp} = engine specific impulse, sec
K_0 = $(p/fM_e)^{1/2}$, hr/mile
M_e = weight of the earth, $1.3177(10)^{25}$ lb
M_m = weight of the moon, $1.6204(10)^{23}$ lb
p_0 = semilatus rectum of initial earth satellite orbit, miles
p = semilatus rectum of earth transfer orbit, miles
r_{em} = earth-moon distance, miles
r_{ev} = earth-vehicle distance, miles
r_{mv} = moon-vehicle distance, miles

Presented at the ARS Electric Propulsion Conference, Berkeley, Calif., March 14–16, 1962; revision received November 30, 1962.

* Manager, Mission Analysis and Evaluation, Space Power and Propulsion Section, Spacecraft Department. Member AIAA.

† Applications Analysis Engineer, Space Power and Propulsion Section, Spacecraft Department.

r = vehicle distance from central body, miles
S = radial component of acceleration, miles/hr^2
t = total propulsion time, hr
T = transverse component of acceleration, miles/hr^2
V_e = vehicle velocity with respect to earth
V_m = vehicle velocity with respect to moon
V_{me} = moon velocity with respect to earth
ΔV = total characteristic velocity, mph
ΔV_m = characteristic velocity of lunar capture phase, mph
W_e = propulsion system weight, lb
W_{gc} = guidance and control systems weight, lb
W_{pc} = power conditioning system weight, lb
W_{pl} = payload weight, lb
W_{pp} = propellant weight, lb
W_{ps} = power conversion system weight, lb
W_{pt} = propellant storage and feed system weight, lb
W_s = structural weight of spacecraft, lb
W_0 = initial system weight, lb
α = moon-earth-vehicle angle at t_2
ϵ = conversion efficiency
ϕ = true anomaly of earth transfer orbit

Subscripts

1 = end of initial propulsion period
2 = end of intermediate coasting period
3 = beginning of lunar capture propulsion period
4 = end of lunar capture propulsion period

A LARGE scale operation involving manned lunar exploration and colonization will require continuous transportation of large quantities of men, machinery, and supplies from the earth to the moon with periodic return of personnel to the earth. The magnitude of the program will place a premium upon the ability to achieve improved payload fractions for the various propulsion operations and on the ability to recover and re-use all equipment orbited from the earth.

This paper will illustrate that electrical propulsion can be used in a lunar transport or ferry role[1] to provide extremely attractive transportation system characteristics. This role is visualized primarily as a logistic support function for the transportation of machinery and supplies. The suitability of electrical propulsion for personnel transportation will be dependent upon shielding requirements for protecting personnel from Van Allen and solar flare radiation during the extended propulsion periods required.[2] This last item is, however, beyond the scope of this paper.

Vehicle, power, and propulsion system characteristics expected for the 1 to 10 Mw range in the 1970 to 1980 time period will be identified. These data will be used to generate typical trajectory characteristics and requirements and to prepare parametric mission performance curves for both one-way and multitrip ferry missions. The resulting data will be evaluated in terms of their suitability for the performance of the desired logistic support function.

System Characteristics

Boost vehicles of the Saturn C-5 or Nova size can be expected to be available for operational use in the 1970 to 1980 time period. In order to provide effective utilization of the earth orbital payload capability of such systems, nuclear electric powerplants and electrical propulsion systems of the 1 to 10 Mw power range will be required.

Nuclear-mechanical power conversion systems appear to offer the most promise for the 1 to 10 Mw power range in the near future. Such systems are currently under development in the 30-kw size[3] and in the planning phase in the 300 kw to 1 Mw size. Additional research and component development is in progress toward the solution of problems associated with the development of megawatt and larger power systems. Although the 30-kw Snap 8 power conversion system is expected to have a specific weight of 50 to 70 lb/kw, substantial

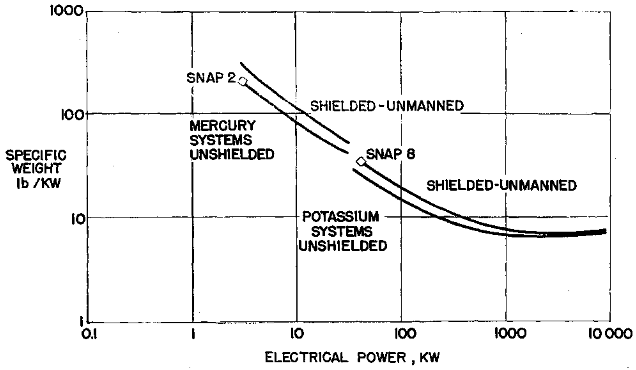

Fig. 1 Specific weight of nuclear mechanical power conversion systems

improvement is expected as power level is increased. Figure 1 illustrates the expected trend in power conversion system specific weight as power rating is increased. These improvements are predicated on reduced reactor specific weight and on the use of higher temperature alkali metal working fluids and containment materials as power level is increased. A power supply specific weight of 7 lb/kw has been assumed to be characteristic of the 1 to 10 Mw power range for the purposes of this study.

Experimental 30-kw thermal arc jet performance indicates that specific impulse levels as high as 1750 sec should be obtainable by the 1970 to 1980 time period. Techniques for extending this technology to engines up to the 500-kw size are being studied. It is expected that the most efficient engine size may be, however, in the 300 to 400 kw range. If this is the case, the desired higher power systems can be obtained by clustering engine modules. Typical thrust capabilities are illustrated in Fig. 2 by engine power requirements per pound of engine thrust as a function of specific impulse. Note that the arc jet operates in the range of 20 to 100 kw/lb of thrust. The engine is expected to weigh about 0.2 lb/kw of power.

Current ion engine technology appears to offer efficient operation over the specific impulse range of 5000 to 10,000 sec. Applied research programs in process offer the promise of extending this operation down to at least 3000 sec. Conversion efficiencies based upon an assumed propellant utilization efficiency of 90% and an overall engine loss of 125 ev/ion can be obtained from the equation

$$\epsilon = 0.90 \left[\frac{6.6(10)^{-5} I_{sp}^2}{125 + 6.6(10)^{-5} I_{sp}^2} \right] \tag{1}$$

The resulting power-to-thrust ratios obtained from Eq. (1) are also illustrated in Fig. 2 as a function of specific impulse. An engine weight of 300 lb/lb of thrust has been assumed to be representative of ion engine characteristics.

The major auxilliary systems will include the propellant storage system, power conditioning equipment, and the guidance and control system. The hydrogen storage system

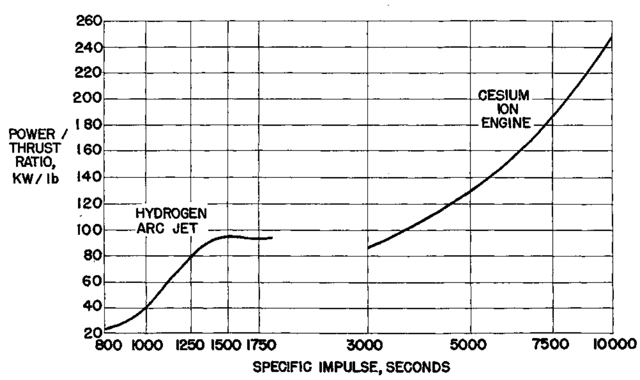

Fig. 2 Thrust capabilities of electric propulsion systems

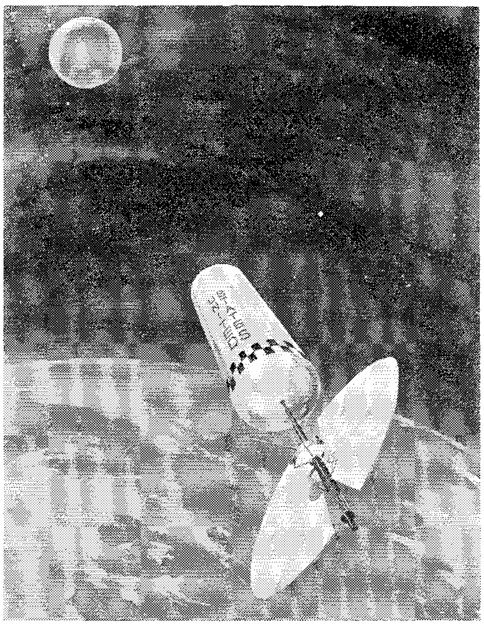

Fig. 3 1-Mw ion propelled space vehicle

for the arc jet will use a double-walled cylindrical pressure vessel with hemispherical ends. Thermal insulation will be provided by a multilayer sheath of aluminum foil wrapped around the outside of the pressure vessel.[4] The system will be designed to permit hydrogen boil-off at the rate required to feed the thermal arc engine. The storage system weight is estimated to be 20% of the propellant weight required. The higher density of the cesium propellant required for ion engine propulsion and the elimination of cryogenic storage requirements will result in a propellant storage system weight of 6% of the total propellant weight. The power conditioning equipment will include the power transmission lines from the power conversion system to the engine, switchgear, controls, starting devices, and any requirements for power transformation or rectification. A weight allowance of 3 lb/kw was assumed. Vehicle guidance and control requirements were assumed to weigh 0.3% of the initial orbital vehicle weight.

The overall space vehicle configuration will be established primarily by the power conversion system configuration and propellant storage requirements. Figure 3 illustrates one approach to a 1-Mw ion-propelled space vehicle. The cesium storage tank is located in the center of the power conversion system radiator. A flat disk configuration is used for the radiator in order to permit waste heat radiation from both sides and to minimize the danger of nuclear radiation being reflected from the radiator to radiation-sensitive elements of the payload. The individual paddle elements of the radiator are stored in a compact cylindrical configuration during launch by feathering the elements, stacking them together, and

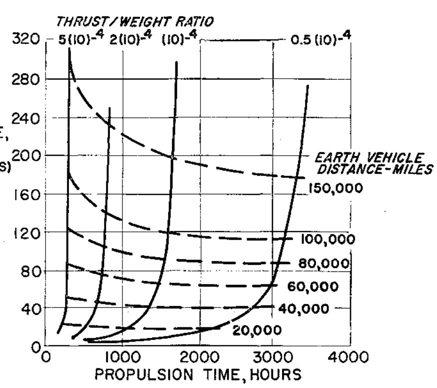

Fig. 4 Transfer trajectory characteristic; specific impulse of 5000 sec

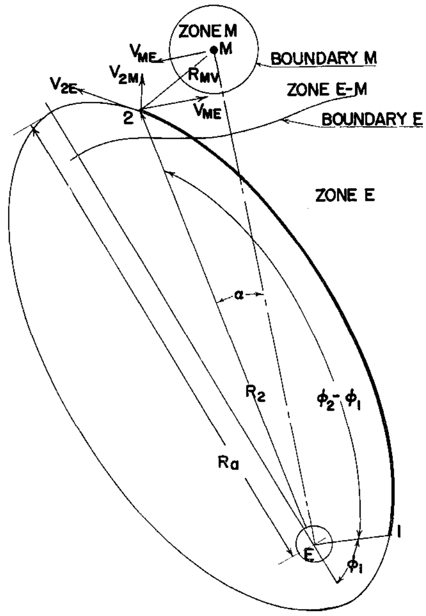

Fig. 5 Intermediate coasting phase

then rotating the assembly into the axial direction. The engines are located above and below the propellant tank and in close proximity to the turbogenerator unit. The reactor is located at the end of the vehicle and is separated from the remainder of the spacecraft by a shadow shield. The payload container is located at the opposite end of the vehicle. Although a 1-Mw thermal arc vehicle would require a substantially greater volume for hydrogen storage, the basic concept would be retained.

A structural weight allowance for the vehicle equal to 5% of the combined power conversion, power conditioning, propulsion, and guidance system's weight was assumed.

Basic Mission Profile

Initial Propulsion Phase

The spacecraft will be injected into an initial earth satellite orbit by a booster of the Saturn C-5 or Nova class. An initial 300-mile circular orbit about the earth has been assumed. During the initial electrical propulsion period, this orbit is converted into an elliptical transfer trajectory that will permit the spacecraft to reach the gravitational sphere of influence of the moon. Transverse thrust orientation has been used for this phase of the mission.[5]

Transfer trajectory characteristics have been studied with the aid of a computer program derived from the classical variation of parameters technique.[6] Although the program consists of a numerical integration of six orbit parameters in order to treat the problem in three dimensions, only three first-order differential equations need be considered in the analysis of the transfer trajectory. These are the following:

$$dp/dt = 2KrT \tag{2}$$

$$de/dt = K[\sin\phi S + (\cos\phi + \cos E)T] \tag{3}$$

$$d\phi/dt = (p/Kr^2) - (K/e)\{-\cos\phi S + \sin\phi[1 + (r/p)]T\} \tag{4}$$

where

$$\cos E = \frac{e + \cos\phi}{1 + e\cos\phi} \qquad r = \frac{p}{1 + e\cos\phi}$$

$$K = \left(\frac{p}{fM}\right)^{1/2} \tag{5}$$

The results of the computer calculations indicate that the true anomaly ϕ varies very slowly and can be assumed to be constant in a first approximation. Retaining only the transverse acceleration term, Eq. (4) then can be combined with Eqs. (5) and rewritten as

$$e = \left(\frac{T}{fM}\right) \frac{p^2 \sin\phi(2 + e \cos\phi)}{(1 + e \cos\phi)^3} \tag{6}$$

Equation (6) then can be differentiated with respect to time and written as

$$\frac{dp}{pde} = \frac{1}{2}\left[\frac{1}{e} + \frac{3 \cos\phi}{1 + e \cos\phi} - \frac{\cos\phi}{2 + e \cos\phi}\right] \tag{7}$$

A second relationship for (dp/pde) can be obtained by dividing Eq. (2) by Eq. (3):

$$\frac{dp}{pde} = \frac{2}{(1 + e \cos\phi)(\cos\phi + \cos E)} \tag{8}$$

Equations (7) and (8) then can be combined and written as

$$3e^3 \cos^4\phi + 14e^2 \cos^3\phi + (18 + e^2)e \cos^2\phi + 4(1 + e^2) \cos\phi - 6e = 0 \tag{9}$$

Although Eq. (9) cannot be solved in closed form, it can be evaluated numerically. At low eccentricities, below 10%, Eq. (9) reduces to the following:

$$\cos\phi = 3e/2 \qquad e < 0.1 \tag{10}$$

Equations (5, 6, and 10) then can be substituted into Eq. (2) and integrated:

$$\frac{1 - 0.214e^2}{p^{1/2}} = \frac{1 - 0.214e_0^2}{p_0^{1/2}} + \frac{g_0 I_{sp}}{fM^{1/2}} \ln\left[1 - \frac{Ft}{W_0 I_{sp}}\right] \tag{11}$$

The resulting Eq. (11) then can be used along with Eqs. (6) and either (9) or (10) to develop transfer trajectory characteristics in parametric form. Figure 4 contains the results of such calculations for a specific impulse of 5000 sec. Apogee altitude is illustrated as a function of propulsion time with lines of constant thrust-weight ratio and orbit altitude indicated.

The cutoff point for the initial propulsion period can be at any time after an apogee altitude of about 200,000 miles has been achieved. Propulsion beyond this point generally will result in an increase in total propulsion requirements and a decrease in the intermediate coasting time and in the sensitivity of the approach orbit to propulsion or guidance errors. An apogee altitude of 238,000 miles has been used as the propulsion cutoff point for this study.

Intermediate Coast Phase

The characteristics of the transfer ellipse required for the intermediate coasting phase are dependent upon the combined earth-moon gravitational field. If the earth is assumed to be the central gravitational body in an inertial coordinate system, the effect of the moon on the vehicle will be the vector difference between its attraction of the vehicle and its attraction of the earth. The moon, therefore, can be said to be the dominant body when its perturbation is greater than the central force of the earth. This will be the case within zone M of Fig. 5 which is bounded by the relationship

$$M_e/r_{ev}^2 = fM_m[(1/r_{mv}^2) - (1/r_{em}^2)] \tag{12}$$

If, on the other hand, the moon is assumed to be the central gravitational body in an inertial coordinate system, the effect of the earth on the vehicle will be the vector difference between its attraction of the vehicle and its attraction of the moon. The earth, therefore, can be considered as the dominant body when its perturbation is greater than the central force of the moon. This will occur within zone E of Fig. 5 which will be bounded by the relationship

$$fM_m/r_{mv}^2 = fM_e[(1/r_{ev}^2) - (1/r_{em}^2)] \tag{13}$$

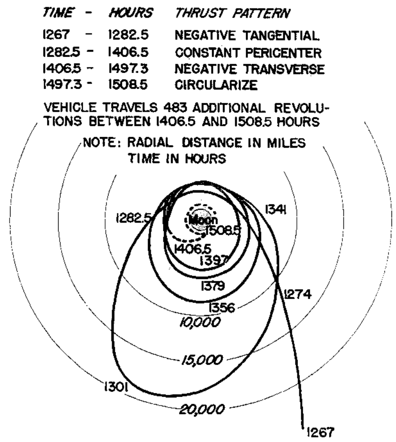

Fig. 6 Lunar capture phase of mission

Within the intermediate zone E-M, either body can be selected as the central body, and the resulting perturbation due to the other body will be less than the central force.

The intermediate coast phase begins at point 1 at the end of the initial propulsion phase and ends at point 2, which must be within zone E-M. In order to minimize overall propulsion requirements, the vehicle-earth-moon angle α was set at about 10 to 11° and r_2 at 220,000 miles at point 2.

The duration of the coasting period was determined from the equations

$$\tan\frac{E_1}{2} = \left(\frac{1 - e_1}{1 + e_1}\right)^{1/2} \tan\frac{\phi_1}{2} \tag{14}$$

$$\tan\frac{E_2}{2} = \left(\frac{1 - e_1}{1 + e_1}\right)^{1/2} \tan\frac{\phi_2}{2} \tag{15}$$

$$t_2 - t_1 = [p_1^3/fM_e(1 - e_1^2)^3]^{1/2}[E_2 - E_1 - e_1(\sin E_2 - \sin E_1)] \tag{16}$$

Coasting periods of 70 to 100 hr were obtained for the range of conditions studied.

Lunar Capture Phase

At point 2, the vehicle velocity relative to the moon V_{2m} must be obtained and used in combination with the vehicle-moon distance r_{mv} to obtain orbit characteristics relative to the moon. This initial orbit will, in general, be a highly elliptical orbit with respect to the moon. Propulsion must be resumed in order to convert the elliptical orbit into the desired low altitude circular orbit about the moon. A typical lunar capture trajectory is illustrated in Fig. 6 after an initial transfer propulsion period of 1191 hr and a coasting period of 76 hr. It is based on an initial thrust to weight ratio of $1.175(10)^{-4}$ and a specific impulse of 1000 sec.

The desired final circular orbit at an altitude of 20 miles was achieved by using tangential, constant pericenter, transverse, and circularizing thrust orientation patterns. These patterns are described in more detail in Ref. 5. This particular sequence was used in order to maintain a continual reduction in both orbit angular momentum and eccentricity throughout the capture maneuver and was necessitated by a pericenter altitude of 2200 miles at lunar approach. With initial altitudes in the range of 10,000 to 15,000 miles, a substantially greater propulsion period will be available before pericenter passage in which proper shaping of the capture orbit can be obtained by tangential thrust steering. Considerably more study is needed, however, in order to obtain a better understanding of the mechanics of the low-thrust lunar capture operation and to identify the most effective steering technique.

The results of the forementioned and similar capture trajectories using other propulsion parameters indicate that the propulsion requirements for the maneuver can be approximated by the equation

$$\Delta V_m = (fM_m/r_4)^{1/2} \pm fM_m/a_3)^{1/2} \quad (17)$$

where the plus sign is used for hyperbolic approach and the minus sign is used for elliptical approach. This terminal propulsion period is, in general, about 15 to 20% of the total propulsion period.

Mission Capabilities

The orbit characteristics of the previous section result in an overall characteristic velocity requirement of approximately 25,700 fps for the mission. This value appears to be relatively insensitive to variations in propulsion system specific impulse or thrust-weight ratio for the range of values investigated. It is, however, somewhat greater than twice the 12,700 fps required to perform an equivalent mission with high-thrust propulsion. This characteristic velocity has been used to generate a series of parametric mission performance curves in order to illustrate the logistic transport capabilities of electric propulsion and to show the trade-offs associated with variations in power-weight ratio, specific impulse, propulsion time, and payload fractions. Data are included for one-way, round-trip, and multitrip missions.

Payload capabilities for one-way lunar missions are illustrated in Fig. 7 as a function of power to initial orbital weight ratio. These data have been generated from the equation

$$\Delta V = -g_0 I_{sp} \ln[1 - (Ft/W_0 I_{sp})] \quad (18)$$

and from the data of Fig. 2. The gross payload represents the weight carried by the spacecraft for injection into orbit about the moon and includes the net payload plus the weight of propulsion and recovery equipment for achieving a soft landing on the surface of the moon. The net payload that can be landed will be about 44% of the gross payload. Gross payload has been obtained from the equation

$$W_{pl} = W_0 - [W_{ps} + W_{pc} + W_e + W_{gc} + W_s] - [W_{pp} + W_{pt}] \quad (19)$$

Parameters of specific impulse and overall propulsion time are indicated in Fig. 7 for both arc jet and ion engine operation. Note that the arc jet represents the only feasible method for achieving the lunar mission when restricted to operation at relatively low power capacities and short propulsion times. If either of these restrictions can be relaxed, substantially greater payload capabilities can be obtained by the use of the ion engine.

Constant propulsion time operation in the ion engine regime exhibits an optimum payload characteristic at increasing specific impulse and propulsion time as power is reduced. This optimum corresponds approximately to the point where the power and propulsion system group weight is equal to the propellant and propellant storage system group weight. No such optimum exists in the arc jet regime.

Round-trip mission capabilities have been generated from the basic one-way mission by trading off payload for propellant in order to complete the return trip. The payload is assumed to be left in a 20-mile circular orbit about the moon and the spacecraft returned to its initial 300-mile circular orbit about the earth. Characteristic velocity requirements for the return trip were assumed to be identical to those of the outbound leg. Payload capabilities for the round trip are illustrated in Fig. 8. The net effect has been a 4 to 5% reduction in payload capabilities and a 300 to 500 hr increase in propulsion time requirements.

Substantially greater payload capabilities can be achieved by re-using the returned spacecraft to conduct additional ferry operations. The spacecraft was assumed, therefore, to be refueled and refitted with an additional payload module after its return to the initial earth satellite orbit. Somewhat larger payload and propellant modules can be supplied to the spacecraft for the subsequent missions if the same booster configuration is used. It should be emphasized, however, that one boost vehicle is required per trip. The number of round-trip missions which can be scheduled with a single spacecraft will depend upon the total operating life capabilities of power, propulsion, and associated subsystems. A capability for 10,000 hr of operation has been assumed for this study.

The data of Fig. 8 have been used to generate payload capabilities for a multitrip mission of 10,000-hr duration. Results are illustrated in Figs. 9 and 10. Figure 9 contains ion engine capabilities when used with a boost vehicle of the Nova size which is assumed to be capable of an orbital payload of 400,000/launch. Payload capabilities for 2 to 5 trip missions are indicated. Note that payload capability appears to be maximized by the use of specific impulse levels within the 6000 to 10,000 sec range. It should be noted that the average payload per trip is decreasing as the number of trips per mission is increased. This is because of the increased weight requirements associated with the higher powered systems needed for completing each trip within a shorter time period.

Comparable logistic payload capabilities are tabulated on Fig. 9 for liquid hydrogen-liquid oxygen chemical rocket and liquid hydrogen nuclear rocket propulsion systems. These data can be used to evaluate the overall economics associated with this operation and to identify the most economical approach to be pursued. This can be accomplished by identifying development, procurement, and operational costs associated with the number of launch pads, boost vehicles, power conversion systems, propulsion systems, and spacecraft asso-

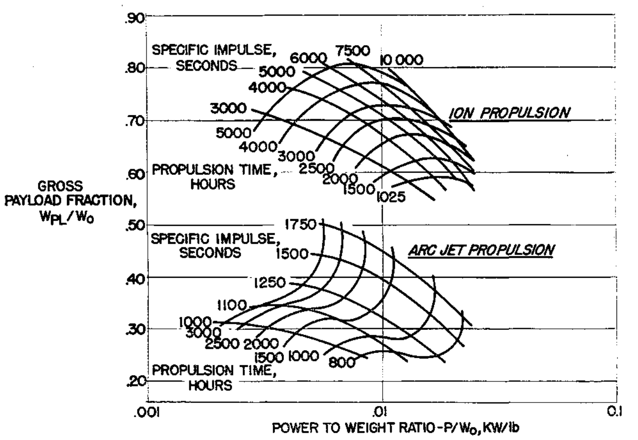

Fig. 7 Payload capabilities for one-way lunar missions

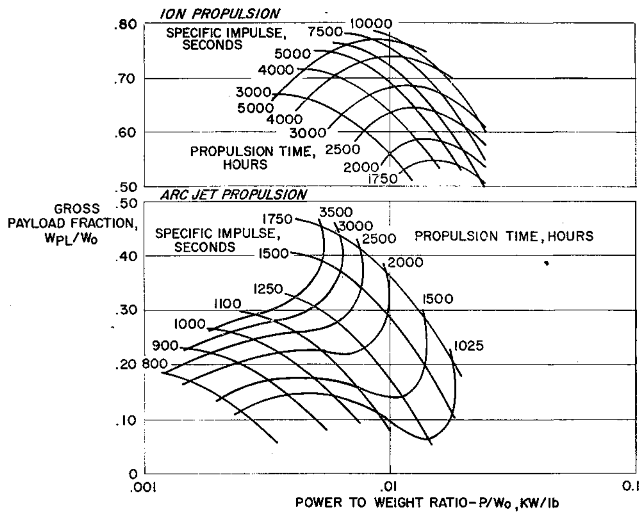

Fig. 8 Payload capabilities for round-trip lunar mission

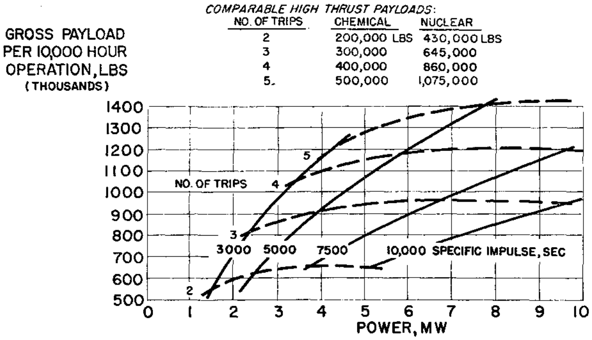

Fig. 9 Payload capabilities for multitrip lunar missions; ion propulsion; 400,000 lb/launch

ciated with a specific logistic payload capability. It would appear, however, that the power conversion system-ion propulsion approach can compete effectively with the chemical and nuclear rocket approach for this type of application.

Similar payload capabilities are illustrated in Fig. 10 for the arc jet engine. These data are characterized by a much more significant reduction in average payload per trip as the number of trips per mission is increased. Payload capabilities of the arc jet for a comparable power rating and number of trips are inferior to those of the ion engine except for the low power-fast trip regime. For the same number of trips, the arc jet capability is slightly better than that of a chemical rocket but poorer than that of a nuclear rocket. Although any final conclusion should be based on the economics of the situation, the foregoing arc jet performance appears to be disappointing in relation to the multitrip missions.

Although arc jet performance, by itself, does not appear to be competitive with nuclear and ion propulsion, it is possible that combined arc jet-ion propulsion on the same spacecraft may permit more effective logistic capabilities for the low power regime. This subject must be investigated in more detail by subsequent studies.

Conclusions

The suitability of electrical propulsion systems of the 1 to 10 Mw size for providing a logistic support capability for lunar exploration has been studied. Although final evaluation of such suitability should be based upon economic considerations as well as on technical considerations, electrical propulsion does appear to offer substantial improvements in payload capabilities over conventional chemical rocket and nuclear rocket propulsion systems.

For one-way lunar missions, payload capabilities with arc jet propulsion are superior when external considerations restrict operation to low power operation with short propulsion

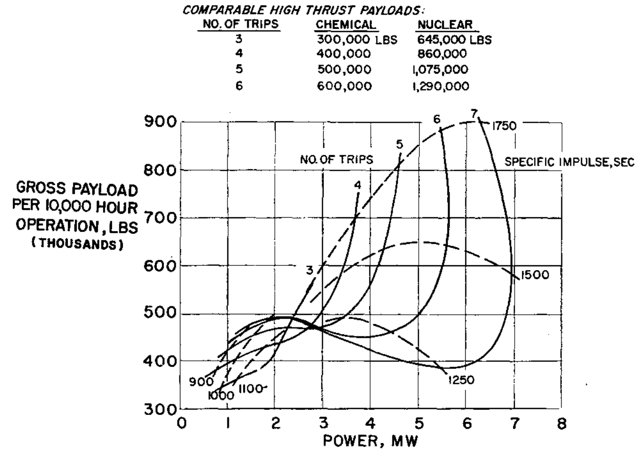

Fig. 10 Payload capabilities for multitrip lunar missions; arc jet propulsion; 400,000 lb/launch

periods. If either the power level restriction or the propulsion time restriction can be relaxed, substantially greater payload capabilities can be obtained with ion propulsion.

Substantial increase in payload capabilities per trip is obtained by re-using the returned spacecraft for a second mission. For a constant system operating life of 10,000 hr, multitrip missions in excess of two trips will result in a decrease in average payload per trip. The total cost may, however, be more attractive than the cost associated with replacing the spacecraft after every second trip.

Ion engine payload capabilities in the 6000 to 10,000 sec regime are considerably more attractive than either chemical or nuclear propulsion for multitrip missions involving a comparable number of launchings. Arc jet propulsion is superior to chemical propulsion for multitrip missions of three or less trips but inferior to those of nuclear propulsion.

References

[1] Stuhlinger, E., "How useful are low-thrust space vehicles," Astronautics **5,** 24–26, 95–97 (February 1960).

[2] Babinsky, A. D., Del Duca, M. G., and Bond, A. F., "The radiation problem in low-thrust space travel," ARS Preprint 989-59 (November 1959).

[3] Hayes, R. J., "Bringing in electrical propulsion," Astronautics **6,** 26–27, 103–107 (July 1961).

[4] "Arc jet application study," Final Rept. NASA Contract NAS5-1034, General Electric Flight Propulsion Lab. Dept. (September 1961).

[5] Brown, H. and Nelson, J. R., "Thrust orientation patterns for orbital adjustment of low thrust vehicles," ARS J. **30,** 635–637 (1960).

[6] Moulton, F. R., *An Introduction to Celestial Mechanics* (MacMillan Co., New York, 1914), pp. 321–405.